



AFRL-RY-WP-TR-2010-1116

A PRELIMINARY INVESTIGATION INTO THE EFFECTS OF HIGH-POWER ILLUMINATION ON OPTICAL PHASED ARRAYS

Bert Whitaker

OptiMetrics, Inc.

Scott R. Harris

Flatiron Research, LLC

MARCH 2010

Interim Report

Approved for public release; distribution unlimited.

See additional restrictions described on inside pages

STINFO COPY

**AIR FORCE RESEARCH LABORATORY
SENSORS DIRECTORATE
WRIGHT-PATTERSON AIR FORCE BASE, OH 45433-7320
AIR FORCE MATERIEL COMMAND
UNITED STATES AIR FORCE**

NOTICE AND SIGNATURE PAGE

Using Government drawings, specifications, or other data included in this document for any purpose other than Government procurement does not in any way obligate the U.S. Government. The fact that the Government formulated or supplied the drawings, specifications, or other data does not license the holder or any other person or corporation; or convey any rights or permission to manufacture, use, or sell any patented invention that may relate to them.

This report was cleared for public release by the USAF 88th Air Base Wing (88 ABW) Public Affairs Office (PAO) and is available to the general public, including foreign nationals. Copies may be obtained from the Defense Technical Information Center (DTIC) (<http://www.dtic.mil>).

AFRL-RY-WP-TR-2010-1116 HAS BEEN REVIEWED AND IS APPROVED FOR PUBLICATION IN ACCORDANCE WITH ASSIGNED DISTRIBUTION STATEMENT.

*/Signature//

TIMOTHY M. FINEGAN
Project Engineer
Electro-optical Combat ID Technology
Branch
Electro-optical Sensor Technology Division

//Signature//

ROBERT J. FELDMANN, Chief
Electro-optical Combat ID Technology
Branch
Electro-optical Sensor Technology Division

//Signature//

BRIAN C. FORD, Col, USAF
Electro-optical Sensor Technology Division
Sensors Directorate

This report is published in the interest of scientific and technical information exchange, and its publication does not constitute the Government's approval or disapproval of its ideas or findings.

*Disseminated copies will show “//Signature//” stamped or typed above the signature blocks.

REPORT DOCUMENTATION PAGE

Form Approved
OMB No. 0704-0188

The public reporting burden for this collection of information is estimated to average 1 hour per response, including the time for reviewing instructions, searching existing data sources, gathering and maintaining the data needed, and completing and reviewing the collection of information. Send comments regarding this burden estimate or any other aspect of this collection of information, including suggestions for reducing this burden, to Department of Defense, Washington Headquarters Services, Directorate for Information Operations and Reports (0704-0188), 1215 Jefferson Davis Highway, Suite 1204, Arlington, VA 22202-4302. Respondents should be aware that notwithstanding any other provision of law, no person shall be subject to any penalty for failing to comply with a collection of information if it does not display a currently valid OMB control number. **PLEASE DO NOT RETURN YOUR FORM TO THE ABOVE ADDRESS.**

1. REPORT DATE (DD-MM-YY) March 2010			2. REPORT TYPE Interim		3. DATES COVERED (From - To) 13 September 2004 – 01 January 2005	
4. TITLE AND SUBTITLE A PRELIMINARY INVESTIGATION INTO THE EFFECTS OF HIGH-POWER ILLUMINATION ON OPTICAL PHASED ARRAYS					5a. CONTRACT NUMBER In-house	
					5b. GRANT NUMBER	
					5c. PROGRAM ELEMENT NUMBER 62204F	
6. AUTHOR(S) Bert Whitaker (OptiMetrics, Inc.) Scott R. Harris (Flatiron Research, LLC)					5d. PROJECT NUMBER 2003	
					5e. TASK NUMBER 11	
					5f. WORK UNIT NUMBER 200311SW	
7. PERFORMING ORGANIZATION NAME(S) AND ADDRESS(ES) OptiMetrics, Inc. 3115 Professional Drive Ann Arbor, MI 48104-5131			8. PERFORMING ORGANIZATION REPORT NUMBER Flatiron Research, LLC AFRL-RY-WP-TR-2010-1116			
9. SPONSORING/MONITORING AGENCY NAME(S) AND ADDRESS(ES) Air Force Research Laboratory Sensors Directorate Wright-Patterson Air Force Base, OH 45433-7320 Air Force Materiel Command United States Air Force					10. SPONSORING/MONITORING AGENCY ACRONYM(S) AFRL/RYJM	
					11. SPONSORING/MONITORING AGENCY REPORT NUMBER(S) AFRL-RY-WP-TR-2010-1116	
12. DISTRIBUTION/AVAILABILITY STATEMENT Approved for public release; distribution unlimited.						
13. SUPPLEMENTARY NOTES PAO Case Number: 88ABW 2010-2483; Clearance Date: 07 May 2010. This report contains color. Research on this report was completed in 2005.						
14. ABSTRACT The phase-vs.-voltage characteristics of liquid-crystal phase retarders and optical phased arrays (OPAs) were measured while the devices were exposed to high-power-CW-laser radiation at 1.08μm. The results indicate that as the applied CW power is increased, the available phase-modulation depth of the devices is reduced, presumably due to heating. In addition, transient experiments where the high-power laser was turned on and off indicate that the particular liquid crystal on silicon (LCoS) OPAs we examined have a thermal time constant of around 20 seconds. Microscopic examination of the liquid-crystal devices indicates that there is no apparent damage to the bulk materials used in the device, although most of the devices appear to have suffered from liquid-crystal migration that is presumably due to thermal expansion and contraction.						
15. SUBJECT TERMS beam steering, optical phased array, OPA, wave plates, phase retarders, phase shifters, liquid crystal, LCoS, thermal damage, laser damage, DC reset, petrographic						
16. SECURITY CLASSIFICATION OF:			17. LIMITATION OF ABSTRACT: SAR	18. NUMBER OF PAGES 24	19a. NAME OF RESPONSIBLE PERSON (Monitor) Timothy M. Finegan 19b. TELEPHONE NUMBER (Include Area Code) N/A	
a. REPORT Unclassified	b. ABSTRACT Unclassified	c. THIS PAGE Unclassified				

Table of Contents

List of figures.....	iv
List of tables.....	iv
1. Introduction.....	1
2. Experimental setup.....	2
3. Results.....	4
3.1. Reduction of phase modulation under high-power illumination.....	4
3.2. Thermal transients.....	4
3.3. Heating.....	4
3.4. Images using crossed polarizers.....	7
3.5. Damage.....	9
4. Thermal modeling.....	10
5. Conclusions.....	13
6. Acknowledgements.....	14
List of acronyms.....	15

List of figures

figure 1 -- Simplified cross section of a liquid crystal optical phased array.....	1
figure 2 -- Schematic diagram of the high-power LCOPA test setup.....	1
figure 3 -- Schematic diagram of the layers in an liquid crystal on silicon device.....	3
figure 4 -- Transmission curves as a function of applied laser power.....	5
figure 5 – Thermal-cooling transient in an LCOPA when illumination is turned off.....	5
figure 6 -- Thermal heating transient in an LCOPA when illumination is turned on.....	6
figure 7 – Phase-vs.-voltage characteristics of a phase shifter undergoing heating.....	6
figure 8 -- A series of images showing the effects of increasing the CW power level	8
figure 9 -- Defect in liquid crystal produced with drive voltage by switching off the laser.....	9
figure 10 -- Microscopic images of a BNS OPA before and after all experiments.....	9
figure 11 -- Simplified heat profile in an LCOPA with heat addition occurring in a thin layer...	12

List of tables

Table 1 -- Thermal conductivity for materials in a typical LCOPA.....	11
Table 2 – Required absorption for a 100-degree-C temperature rise across an LCOPA layer.....	11

1. Introduction

Liquid-crystal optical phased arrays (LCOPA's) have been the subject of a large amount of development work over the past decade and are being proposed as an integral part of non-mechanical-beam-steering systems. The basic arrangement of an LCOPA is shown in figure 1. The LCOPA is a thin layer of liquid-crystal (LC) material sandwiched between two substrates. Both substrates can be transparent, in which case the LCOPA is operated as a transmissive device; or one of the substrates can be reflective and the LCOPA is consequently used in a reflective fashion. Since the liquid-crystal material is birefringent and has dielectric anisotropy, the local index of refraction is adjustable by applying different voltages to an array of electrodes. In a reflective device, the electrodes are typically aluminum and are often part of a very-large-scale-integration (VLSI) silicon backplane that includes other electrical functionality. The window on a reflective device is typically fused silica and is coated with a transparent, conductive oxide (TCO) such as Indium Tin Oxide (ITO). Transmissive devices must use a patterned array of TCO electrodes on the addressing layer.

Almost all of the work with LCOPA's to date has focused on the demonstration of a variety of optical configurations and applications at low optical powers. Typically experiments with OPA's are performed using diode lasers or low-power, gas lasers (Helium-Neon or Argon, for example). Since the eventual goal is to incorporate LCOPA's into a variety of high-power laser systems such as military, active electro-optical systems and industrial applications, we have begun to examine the properties of liquid-crystal devices when used with high-power pulsed and continuous-wave (CW) lasers.

This paper presents the results of some initial experiments aimed at examining the ability of current optical phased array technology to manipulate high-power-CW-laser energy.



Figure 1: Simplified cross section of a liquid-crystal optical phased array.

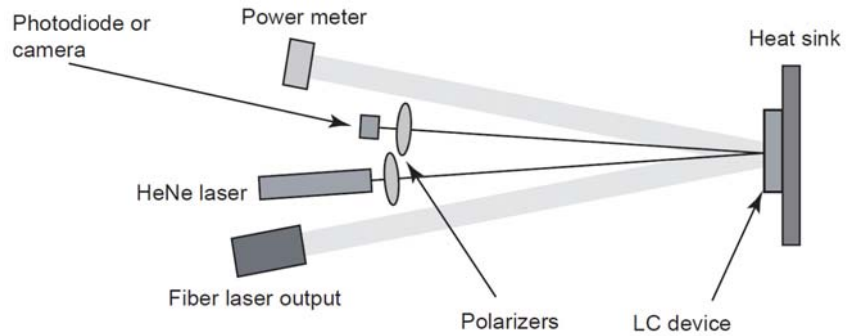


Figure 2: Schematic diagram of the high-power LCOPA test setup.

2. Experimental setup

The setup used in these experiments is shown in figure 2. The liquid-crystal devices under test are mounted on an aluminum block with an adhesive, thermally conductive compound. The block is cooled with circulating water. The aluminum block could also be heated with a resistive element controlled by an Omega CN76000 temperature controller so that the effects of a simple heating could be compared to that induced by laser exposure. All of the devices used in these experiments were reflective and produced by Boulder Nonlinear Systems (BNS). An IPG Photonics Ytterbium fiber laser (model YLR-100-LP) was used to apply high-power-CW-laser energy to the LC device under test. The fiber laser produced a TEM00 beam at 1080 nm, and the power was continuously adjustable between 0 and 100 Watts. The beam diameter was 5 mm (defined by the $1/e^2$ intensity). The output polarization of the laser was linear, but the orientation was not controlled for these experiments since the laser was only used to provide a high-power loading on the LCOPA. The fiber laser was aimed at the center of the liquid-crystal device under test at an angle of approximately 10 degrees to its surface normal. The high-power beam was terminated into a Molelectron PM300F-50 laser-power-meter head. The laser-power meter was used to monitor the power reflected from the LC device and to verify that it was comparable to the applied power indicated by the internal monitor in the laser source.

The $1/e^2$ diameter of 5 mm results in a peak intensity for a given laser power that is $10.21/cm^2$ times the applied power in Watts. Therefore, one Watt of laser power results in a peak intensity of 10.2 Watts/cm². A peak intensity of 100 Watts/cm² corresponds to a total applied power of only 9.8 Watts. In general, the peak power in a Gaussian beam is given by $2P/\pi\sigma^2$, where P is the total power in the beam, and σ is the $1/e^2$ radius of the intensity profile.

In these experiments, the transmission through crossed polarizers was used to infer the phase-shifting behavior of the devices. The laser source was an approximately 1 mW, green helium-neon (HeNe) laser operating at 543 nm. The HeNe was arranged so that the laser was incident on the LC device at an angle of approximately 1.8 degrees to its surface normal. The first polarizer was adjusted so that the light incident on the LC device was oriented at roughly 45 degrees relative to its optical axis. The reflected light passed through a second polarizer oriented at approximately -45 degrees before hitting a photodiode (Thorlabs model DET210). The output of the photodiode was conditioned by a Stanford Research Systems model SR570 low noise current preamplifier. The voltage traces from the amplifier were displayed and recorded with a Tektronix TDS3054 oscilloscope.

The variations in the transmitted intensity are proportional to the cosine of the actual phase shift produced by the LC device. Although the intensity data can be converted to phase data, for many experiments it is sufficient to simply count the number of cycles in the transmitted intensity to determine the total phase-shifting range of the device under test.

Two different types of devices were used in these experiments. The first device was a reflective-liquid-crystal cell, which was operated as a simple phase shifter. The back surface of the cell is fused silica coated with an aluminum electrode layer and covered with a reflective dielectric stack. The front surface was a piece of fused silica with an ITO coating. The liquid-crystal material in the device was BL087. The device was swept through its phase shifting range by a Stanford Research Systems DS345 function generator. The function generator provided a 1kHz square wave that was slowly AM modulated between 0 and 10 volts, peak to peak. The output impedance was set at 50 Ohms.

The second type of device was a BNS, 4096-element optical phased array. This device consists of a VLSI Silicon backplane, a reflective dielectric stack, an LC layer, and an ITO-coated cover glass. A more complete cross section of this device is shown in figure 3. Each electrode on this device is independently controllable and can be used to generate useful phase patterns for beam steering or shaping. However, in order to avoid scattering high-power-laser energy from the fiber laser the OPA's were only operated with all of their electrodes at the same voltage so that the device behaved as a simple phase shifter. Nevertheless, some $1.08\mu\text{m}$ light was observed to diffract (presumably) from the $1.8\mu\text{m}$ -pitch-electrode pattern behind the dielectric reflective coating.

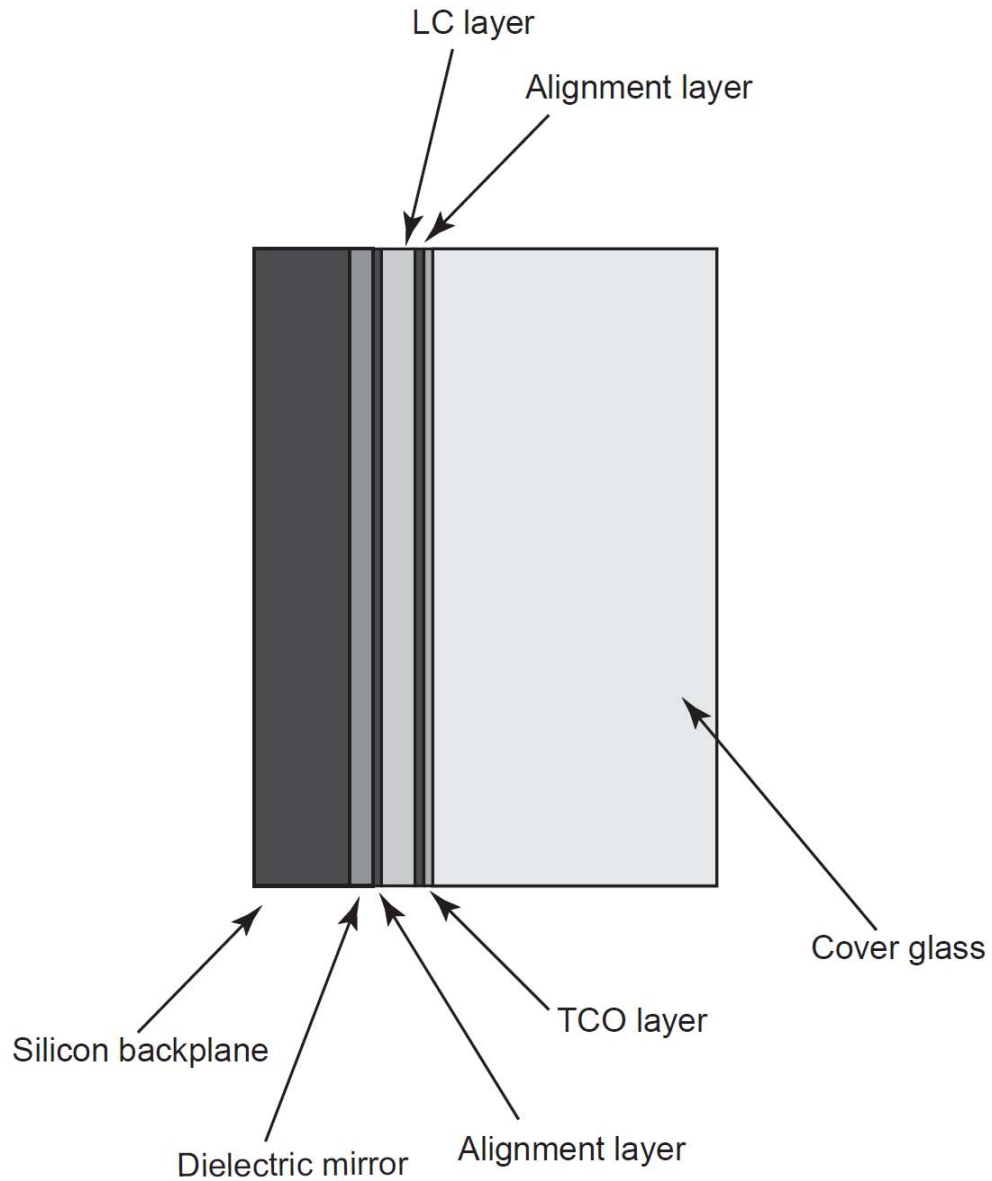


Figure 3: Schematic diagram of the layers in a liquid-crystal-on-silicon device (not to scale).

3. Results

3.1. Reduction of phase modulation under high-power illumination

Figure 4 shows the transmission through crossed polarizers as a spatial light modulator (SLM) is swept through its full voltage range for a spectrum of CW laser power loading conditions. Unfortunately, the oscilloscope was not set to display the data at its full resolution resulting in the relatively noisy curves shown. Nevertheless, it is clear that the phase shift produced by the device decreases monotonically as the applied power loading is increased. This can be observed by noticing that the peaks and troughs in the sinusoidal pattern move to the right as the applied laser power is increased. Comparing the curves that correspond to 0 Watts and 10 Watts (approximately 100 W/cm^2), we can see that the phase-vs.-voltage characteristics of the device are essentially unchanged at this power level.

3.2. Thermal transients

In order to investigate the temporal behavior of the thermal effects in an LCOPA, the transmission curve of an SLM was recorded while the high-power laser was turned on and off. The LCOPA was operated at an intermediate voltage (i.e. the experiments were not performed with the LC in a homogenous alignment.).

Figure 5 shows the transient transmission curve after the high-power illumination of 70 W was interrupted. Clearly it takes several tens of seconds for the device to recover to its room temperature state. The applied voltage on the LC layer in this case was one half of the maximum value (128/255). Figure 6 shows the transient obtained when a high-power illumination of 70 W is instantaneously applied to the device. Again, the time required to reach a steady state is several tens of seconds. In the laser-switching-on experiment, the voltage applied to the device was 173/255 of the maximum voltage. The applied voltage on the LCOPA was chosen to be roughly in the middle of the available range and to produce a large intensity change during the thermal transient.

3.3. Heating

The temperature of a single-pixel, liquid-crystal phase shifter was slowly increased in order to compare the effects of a simple heating to those produced by high-power laser exposure at $1.08\mu\text{m}$. Figure 7 shows the transmission curves of the phase shifter as the temperature was slowly increased. The decrease in phase-shifting ability is qualitatively the same as that observed in the spatial light modulators exposed to high-power-laser energy.

When SLM's and phase shifters were heated to very high temperatures they ceased to operate. In the case of SLM's, any heating above approximately 50 degrees Centigrade rendered the devices non-functional. The mechanism for this effect is currently unknown. Phase shifters were also rendered non-functional when they were heated to excessively high temperatures, but the critical temperature in these cases was 70 degrees Centigrade.

A phase shifter, rendered non-functional by heating, was accidentally exposed to a 0.5-Hz, 10-volt-peak-to-peak signal for four seconds instead of the normal, 1-kHz drive voltage, and it appears that this procedure restored the phase shifter to its original operating condition. This sequence was repeated several times with several different phase shifters, and, in all cases, the low-frequency drive voltage restores thermally “deactivated” devices to normal operation. We speculate that the mechanism for this behavior is related to a change in the liquid-crystal alignment caused by raising the temperature above the clearing point of the liquid crystal. The limitations of the drive electronics for the SLM's prevented us from applying this low-frequency procedure with SLM's that had been heated to excessively high temperatures.

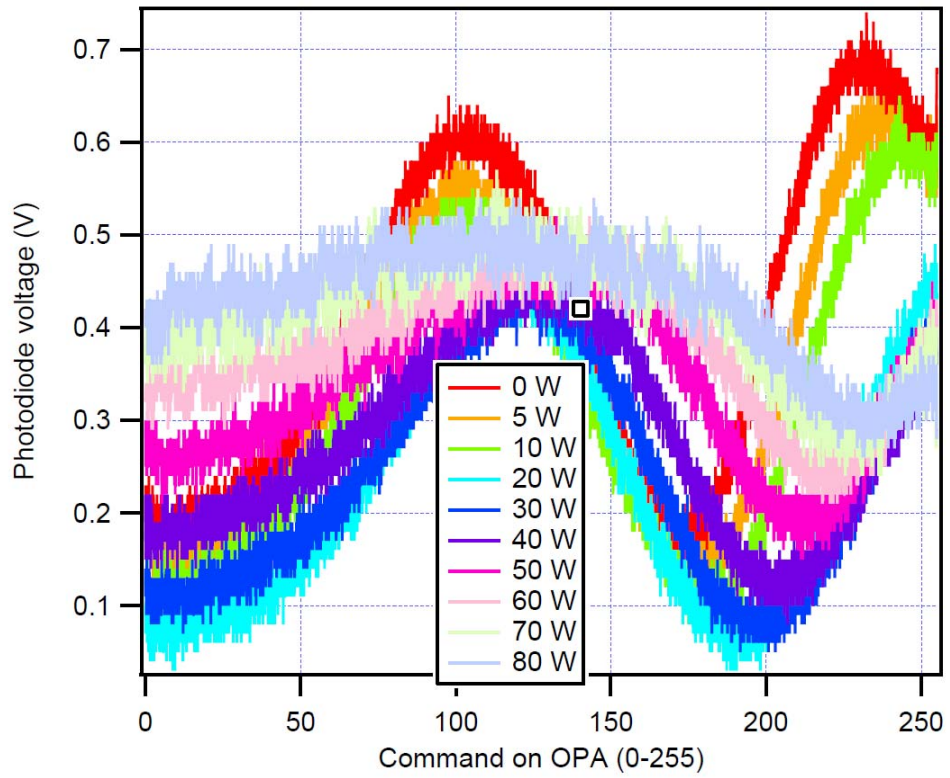


Figure 4: Transmission curves for different applied-laser power levels.

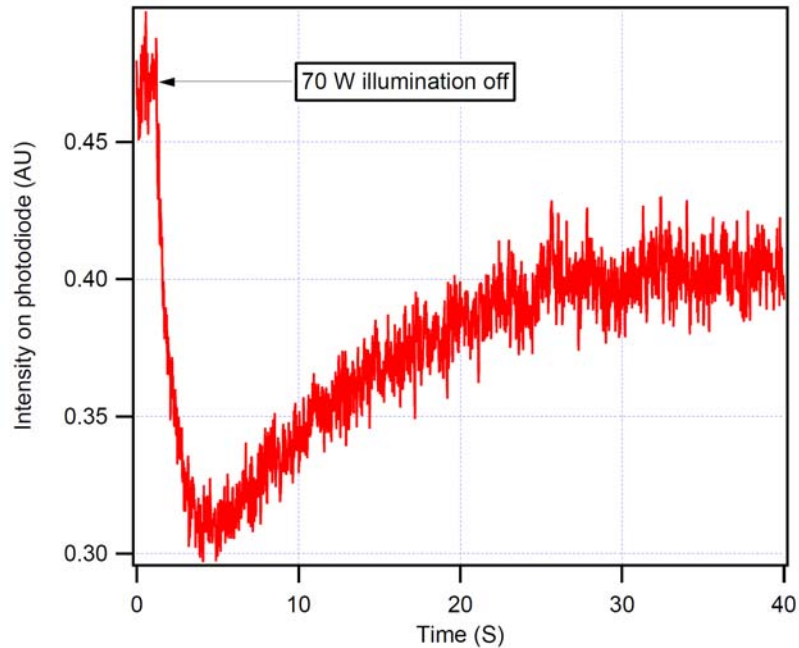


Figure 5: Thermal-cooling transient in an LCOPA when high-power illumination is turned off.

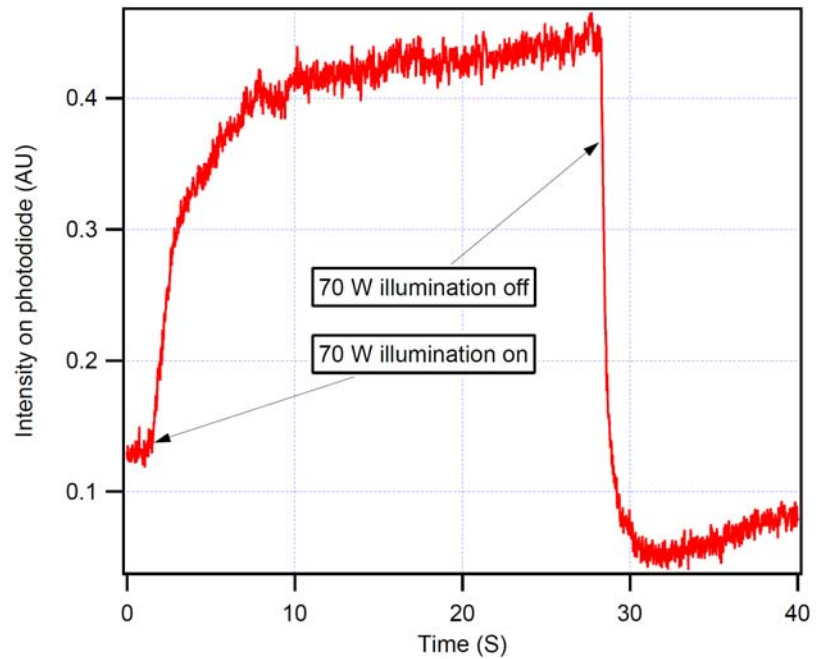


Figure 6: Thermal-heating transient in an LCOPA when high-power illumination is turned on.

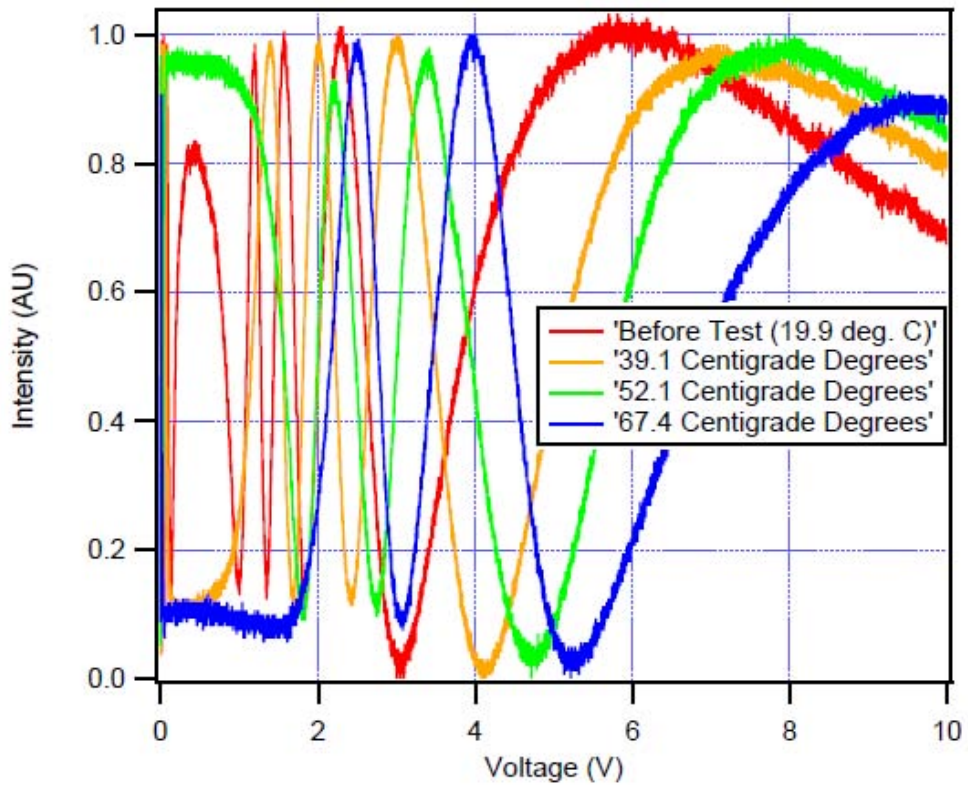


Figure 7: Phase-vs.-voltage characteristics of a liquid-crystal phase shifter undergoing heating.

3.4. Images using crossed polarizers

In addition to quantitatively measuring the phase-vs.-voltage response of the device near the center of the applied high-power-CW-laser beam, qualitative images of the effects of the CW-laser beam were obtained by imaging the phase shifter or OPA under test through crossed polarizers. A short-pass filter (a laser-goggle lens) was placed in front of the camera to block the intense scatter at $1.08\mu m$.

Figure 8 shows a sequence of still images of a phase shifter taken from a video sequence recorded while the CW-laser power was slowly increased to its maximum value. The thermally induced change in birefringence produces a series of concentric interference fringes.

From the images in figure 8, it is clear that the high-power laser is causing a localized reduction in the phase-shifting ability of the device. Real-time-video examination of the device while it was being driven with a periodic signal to produce a periodic phase shift confirms that the central region produces a decreasing phase-shift amplitude as the applied laser power is increased.

When the high-power laser was quickly turned off while the phase shifter was powered, features like that shown in figure 9 persisted in the device. Slowly decreasing the laser power did not produce these defects. Subsequent re-exposure of the spot to high-power-laser energy followed by a slow (several minutes) decrease in the laser power appeared to “repair” the device and eliminate the defect. These defects appear to be domain boundaries produced when a localized part of the liquid-crystal layer is brought above the clearing temperature and then cooled in the presence of an electric field. We speculate that the slow reduction of laser power anneals the defect.

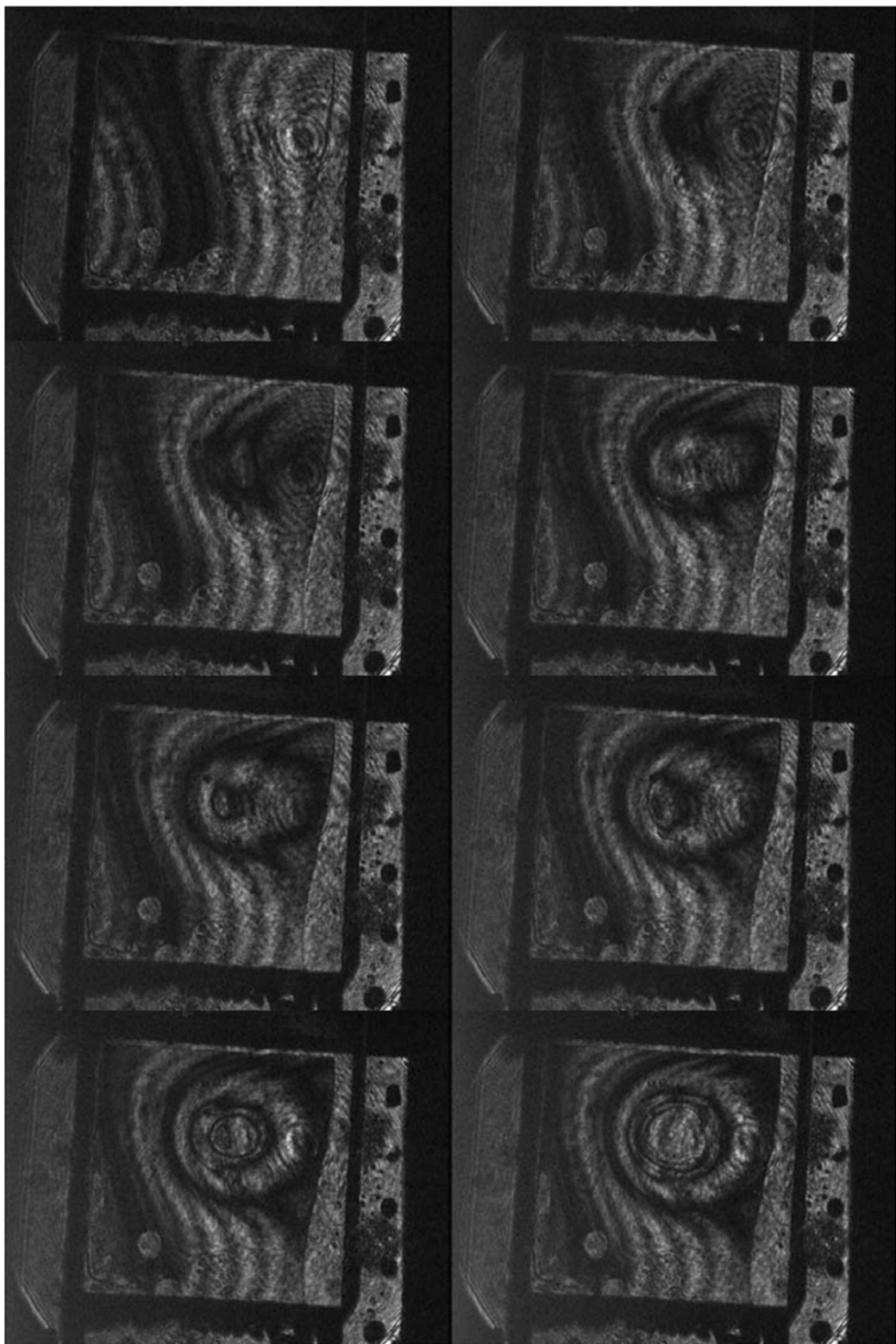


Figure 8: A series of images showing the effects of increasing the CW laser power applied to the liquid crystal device. Laser power levels are 0W, 30W, 40W, 50W, 60W, 80W, 90W, and 100W (left to right, top to bottom).

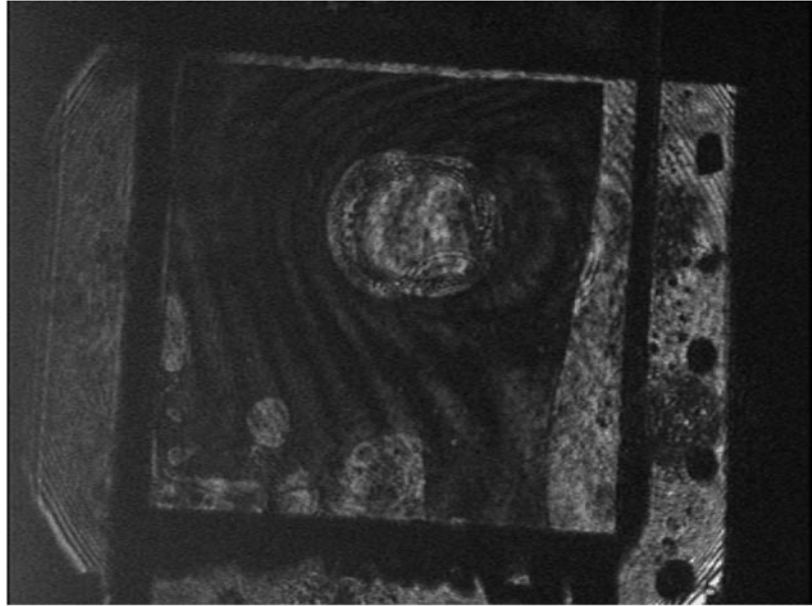


Figure 9: Defect in liquid-crystal layer produced by switching off the high-power-laser illumination while a driving voltage is still applied to the device.

3.5. Damage

The devices examined in this effort exhibited a variety of both permanent and temporary changes when they were exposed to extremes of temperature and laser power. At lower laser powers (corresponding to around 100 W/cm^2), the only changes observed in the devices was minor migration of the liquid-crystal material.

Repeated exposure to high-power-laser energy and thermal cycling of the devices produced significant migration of the liquid-crystal layer. We assume that this movement of the liquid crystal is caused by thermal expansion and contraction. Figure 10 shows the boundary of the liquid-crystal layer in an SLM before and after several exposures to high-power-CW-laser radiation.

We did not visually observe any obvious, visually detectable damage to the cover glass or backplanes in any of the devices examined.



Figure 10: Microscopic images of the lower-right region of a BNS OPA before (left) and after (right) all high-power-CW-laser experiments.

4. Thermal modeling

In order to better understand the thermal behavior of LCOPA's, we will consider a one-dimensional model of heat diffusion in a liquid-crystal device. The temperature distribution in an inhomogeneous, layered material is given by the familiar heat equation shown in equation 1.

$$\sigma \rho \frac{du}{dt} = \frac{d}{dx} \left(K \frac{du}{dx} \right) \quad (1)$$

K is the thermal conductivity of the material, ρ is the density, σ is the heat capacity, and $u(x, t)$ is the temperature distribution. If we restrict our attention to the steady-state temperature distribution in a layered structure composed of homogenous layers, then we find, in regions where no heat is being absorbed, that

$$K \frac{d^2 u}{dx^2} = 0. \quad (2)$$

Equation 2 only admits solutions of the form

$$u(x) = C_1 x + C_2. \quad (3)$$

At each boundary between layers there are two conditions to be satisfied. The first condition is continuity of the temperature distribution. The second condition is that the heat fluxes across the boundary must match. In this model, we will assume that all of the thermal absorption takes place in infinitely thin layers between the material boundaries.

$$\left(K_1 \frac{du}{dx} \right)_{right} - \left(K_2 \frac{du}{dx} \right)_{left} + q_{source} = 0 \quad (4)$$

If we assume that all of the heat deposited in the LC cell is removed through the back plane and that radiation and convection from the front of the device are negligible, then we can arrive at a simple procedure for evaluating the temperature distribution inside the device.

Since no heat can travel to the right and exit through the cell's cover glass, the temperature gradient to the right of the heat absorption must be zero. This implies that the temperature in the cover glass is constant. To the left of the heat source, the slope of the temperature profile is linear and simply given by

$$K \frac{\Delta u}{\Delta L} = Q/A. \quad (5)$$

In other words, the temperature drop across each layer must be that required to cause the deposited heat to flow toward the heat sink. The temperature rise in each layer is proportional to $\Delta L/K$.

For a given layer, the temperature drop will be

$$\Delta u = \frac{\Delta L Q}{KA}, \quad (6)$$

where Q/A is the power deposited in units of W/cm^2 , and ΔL is the thickness of the layer.

Material	Thermal conductivity	Thickness	$\Delta L/K$
LC	$0.2 \text{ W}/(\text{mK})$	$7 \mu\text{m}$	3.5×10^{-5}
Silicon	$138 \text{ W}/(\text{mK})$	$720 \mu\text{m}$	5.2×10^{-6}
Fused Silica	$13 \text{ W}/(\text{mK})$	$2000 \mu\text{m}$	1.5×10^{-4}

Table 1: Thermal conductivity for materials in a typical LCOPA.

Material	Required thermal load for 100 K temperature rise
LC	$286 \text{ W}/\text{cm}^2$
Silicon	$1900 \text{ W}/\text{cm}^2$
Fused Silica	$65 \text{ W}/\text{cm}^2$

Table 2: Required heat absorption for a 100-degree-C temperature rise across a material layer in an LCOPA.

Looking at table 1, it is clear that the temperature rise in the LC layer will dominate the overall temperature rise in the device because the resistance to heat flow in the liquid-crystal layer is about an order of magnitude higher than that of a silicon backplane. The thermal conductivity of the LC layer is estimated to be roughly similar to that of an organic solvent.

The actual thermal loadings (absorbed power, not applied-laser power) required to produce a 100-K temperature rise across a layer in an LCOPA are shown in table 2. The cover-glass layer in the device is the most insulating layer in the LCOPA, but, since it is an adiabatic boundary, it plays no role in determining the internal temperature of the device.

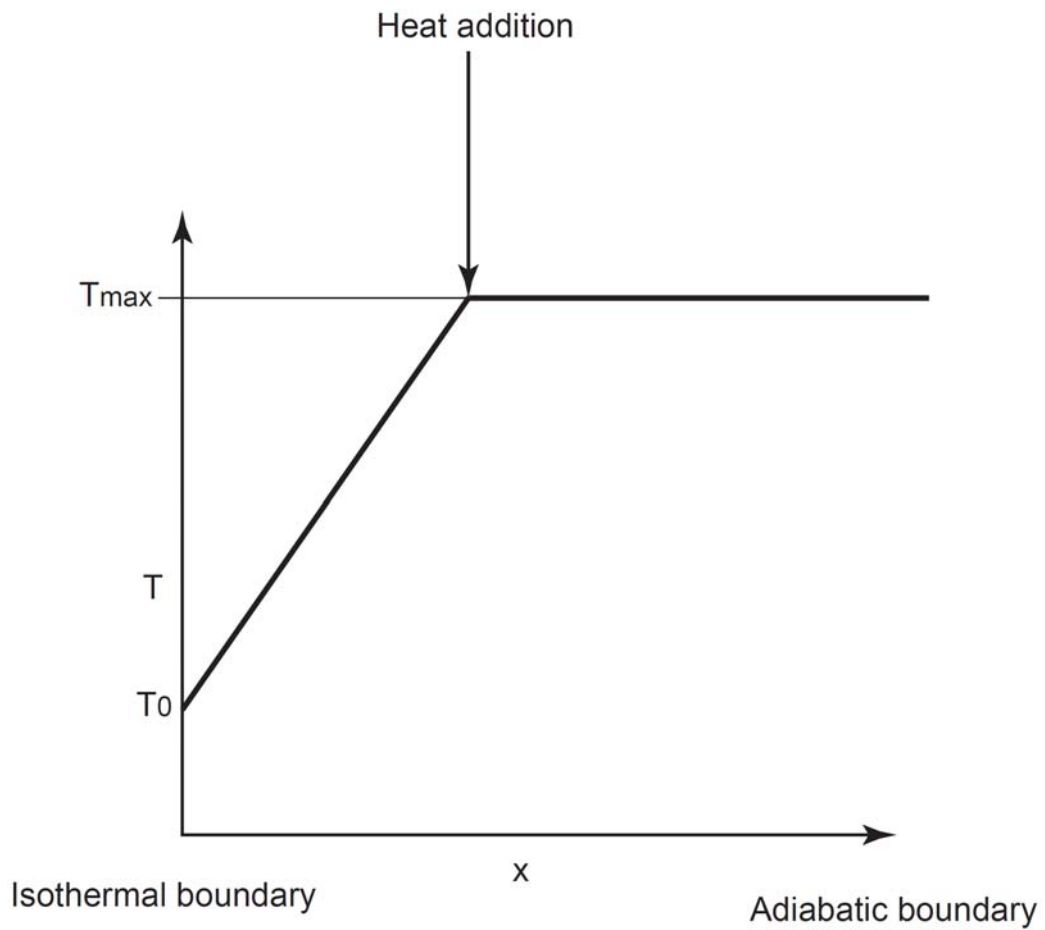


Figure 11: Simplified heat profile in an LCOPA device with one adiabatic boundary, one isothermal boundary, and heat addition occurring in a thin layer.

5. Conclusions

We have demonstrated that reflective, liquid-crystal optical phased arrays can easily operate at CW-laser-intensity levels of up to 100 W/cm^2 without any significant difficulties. At higher power levels, the heating caused by absorption of the laser energy causes two adverse effects. First, the locally elevated temperatures cause a reduction of the liquid-crystal birefringence and eventually drive the liquid-crystal layer to an isotropic state. Secondly, the repeated, extreme heating and cooling cycles caused by the high-power laser appear to cause the liquid-crystal material to migrate inside the device. We speculate that this phenomenon can be controlled with either better seals around the cell edges or a specific design feature that permits the liquid crystal to expand and contract in a reservoir area. Exposure to high temperatures appears to damage the devices in a way that is not currently understood.

Finally, we presented a simple, one-dimensional thermal model for a liquid-crystal optical phased array that allows the estimation of the relative importance of different materials and regions in the device to the temperature distribution within.

6. Acknowledgements

The authors would like to thank Steve Serati, Teresa Ewing, and Jay Stockley of Boulder Nonlinear Systems for their assistance and for supplying us with the SLM's and phase shifters used in these experiments.

List of acronyms

AM: amplitude modulation

BNS: Boulder Nonlinear Systems

CW: continuous wave, usually in reference to lasers, as opposed to pulsed

DC: direct current, as opposed to alternating

HeNe: helium-neon, in reference to the lasing medium of specific lasers

ITO: indium tin oxide

LC: liquid crystal

LCOPA: liquid-crystal optical phased array

LCoS: liquid crystal on silicon

OPA: optical phased array

SLM: spatial light modulator

TCO: transparent, conductive oxide

VLSI: very-large-scale integration